

Supplementary Information for:

Enzymatic activation of cell-penetrating peptides in self-assembled nanostructures triggers fibre-to-micelle morphological transition

Yejiao Shi^a, Yang Hu^b, Guy Ochbaum^c, Ran Lin^b, Ronit Bitton^c, Honggang Cui^b and Helena S. Azevedo^{a*}

^a School of Engineering and Materials Science, Institute of Bioengineering, Queen Mary, University of London, London, E1 4NS, UK

^b Department of Chemical and Biomolecular Engineering, Institute for NanoBioTechnology, Johns Hopkins University, Baltimore, MD 21218, USA

^c Department of Chemical Engineering and the Ilza Katz, Institute for Nanoscale Science & Technology, Ben-Gurion University of the Negev, Beer-Sheva 84105, Israel

* Correspondence Author E-mail: h.azevedo@qmul.ac.uk

Contents:

S1 Chemicals	S2
S2 Methods	
S2.1 Synthesis and Purification of CPPAs.....	S2
.....S2.2 Preparation of CPPA and CPPA _{MMP} Assemblies.....	S3
S2.3 Secondary Structure Characterization.....	S3
S2.4 Critical Aggregation Concentration (CAC) Determination.....	S3
S2.5 Small Angle X-ray Scattering (SAXS) Analysis.....	S3
S2.6 Transmission Electron Microscope (TEM) Imaging.....	S4
S2.7 Zeta-potential Measurement.....	S4
S2.8 MMP-2 Cleavability Evaluation.....	S4
S3 Supporting Figures	
Fig. S1 Chemical structure of the rationally designed CPPA.....	S5
Fig. S2 Characterization of CPPA.....	S5
Fig. S3 Characterization of CPPA _{MMP}	S5
Fig. S4 Characterization of the CPPA degradation fragment.....	S6
.....Fig. S5 MMP-2 cleavage efficiency of CPPA fibers.....	S6
Table 1 Zeta-potential measurements.....	S6
S4 References	S6

S1 Chemicals

Fmoc-amino acids and 4-methylbenzhydrylamine (MBHA) rink amide resin were purchased from Novabiochem. O-benzotriazole-N,N,N',N'-tetramethyl-uronium-hexafluorophosphate (HBTU) was purchased from Carbosynth. Diisopropylethylamine (DIEA), piperidine, dimethylformamide (DMF), dichloromethane (DCM), trifluoroacetic acid (TFA), triisopropylsilane (TIS), diethyl ether, acetonitrile (ACN), palmitic acid, hydrochloric acid (HCl), ammonium hydroxide (NH₄OH), Nile Red and the Kaiser Test Kit were purchased from Sigma-Aldrich and used without further purification. Uranyl acetate was purchased from Agar Scientific.

The active human MMP-2 (CHO cells) was purchased from Merck Millipore (Catalogue Number: PF023-5UG; MW = 62 kDa, Activity $\geq 7.0 \Delta A_{405}$ /hour/ μ g protein in standard thiopeptolide hydrolysis assays).

Milli-Q water was obtained from a Merck Millipore Milli-Q Integral water purification system with a minimum resistivity of 18.2 M Ω .cm.

S2 Methods

S2.1 Synthesis and Purification of CPPAs: The CPPAs used in this work were synthesized by a Liberty Blue automated microwave peptide synthesizer (CEM) on a MBHA rink amide resin using the standard Fmoc solid phase peptide synthesis. Briefly, each of the amino acid coupling cycle was performed with a mixture of Fmoc-amino acid/HBTU/DIEA at a ratio of 4:4:6 relative to the resin. Fmoc deprotections were performed with 20% piperidine in DMF twice for 10 min. The palmitic acid tail was manually coupled under the same condition as the Fmoc-amino acids. The coupling reaction of palmitic acid tail was monitored by the Kaiser Test Kit for free amines. Once all coupling reactions were completed, CPPAs were cleaved from the resin using a mixture of TFA/TIS/H₂O at a ratio of 95:2.5:2.5 for 4 h with simultaneous removal of the protecting groups. The cleavage solution was then collected and excess TFA was removed by rotary evaporation. Cold diethyl ether was added to the obtained viscous solution to precipitate the peptide products, which were then collected, washed again with cold diethyl ether and dried under vacuum overnight. The mass of crude CPPAs was confirmed by Electrospray Ionization Mass Spectrometry (ESI-MS, Agilent). The purification of the CPPAs was performed on an AutoPurification System (Waters) using a preparative reverse-phase C18 column (XBridge, 130 Å, 5 μ m, 30 \times 150 mm, Waters) and a H₂O/ACN (0.1% TFA) gradient. Fractions containing CPPAs were collected automatically when the exact mass signals were detected by the SQ Mass Detector (Waters). The purified CPPAs were then filtered through a PL-HCO₃ SPE syringe column (Agilent) to remove TFA counter-ions, lyophilized and stored at -20 °C for further use. Confirmation of mass and purity of the CPPAs was done by ESI-MS and Alliance HPLC system (Waters) equipped with an analytical reverse-phase C18 column (XBridge, 130 Å, C18, 3.5 μ m 4.6 x 150 mm, Waters).

S2.2 Preparation of CPPA and CPPA_{MMP} Assemblies

CPPA and CPPA_{MMP} assemblies were prepared by dissolving the obtained peptide amphiphile powder to a concentration above the CAC at 200 μ M in Milli-Q water. 0.1 M HCl and NH₄OH solution were added to adjust the pH to 7.4. All the characterizations were performed after 24 h unless otherwise statement.

S2.3 Secondary Structure Characterization: The secondary structure of CPPAs was characterized by circular dichroism (CD) spectrometer. CPPAs were dissolved in Milli-Q water at a concentration of 50 μ M and the pH was adjusted to 7.4 using 0.1 M HCl or 0.1 M NH₄OH solution. The CPPA solutions were then loaded into a 1 mm path length quartz cuvette and the CD spectra were recorded on a Chirascan CD spectrometer (AppliedPhotophysics) from 190 to 280 nm at 25 °C. Background spectrum of the solvent was obtained and subtracted from the sample spectra. The mean residue ellipticity $[\theta]_{\lambda}$ was calculated using the following equation:

$$[\theta]_{\lambda} = \frac{[\theta]_{obs}}{10 \cdot c \cdot l \cdot n}$$

Equation 1

where $[\theta]_{obs}$ is the observed ellipticity at λ in mdeg, c is the concentration of CPPAs in M, l is the light path length of the cuvette in cm, and n is the number of amino acid residues in CPPAs.

S2.4 Critical Aggregation Concentration (CAC) Determination: The CAC of CPPAs was determined based on a hydrophobic solvatochromic dye Nile Red, which exhibits an increased fluorescence intensity and pronounced blue shift when encapsulated into the hydrophobic pocket of the assembled nanostructures¹. Nile Red was dissolved in acetone and aliquoted to eppendorf tubes before being left in dark place at room temperature to form dry films. CPPA aqueous solutions with various concentrations, ranging from 100 nM to 1 mM, were prepared and were then added to the eppendorf tubes to dissolve the Nile Red dry film to a final concentration of 1 μ M. The Nile Red and CPPA mixture solutions were aged overnight in a dark place at room temperature to allow the equilibrium of Nile Red partition between water and the core of the nanostructures. Fluorescence emission spectrum of each sample was recorded on a LS55 fluorescence spectrometer (PerkinElmer) ranging from 580 to 720 nm with an excitation wavelength at 550 nm. The maximum intensity and the corresponding wavelength of each spectrum were determined after subtracted from the blank sample and were then plotted as a function of logarithm CPPA concentration. The CAC could be determined at the point where there is a sharp increase in the fluorescence intensity and a hypochromic shift.

S2.5 Small Angle X-Ray Scattering (SAXS) Analysis: SAXS was used to characterize the shape, size and size distribution of the CPPA assemblies. SAXS measurements were performed using SAXSLAB GANESHA 300-XL. Cu K α radiation was generated by Genix 3D Cu-source and was selected with integrated monochromator and 3 pinholes

collimation. Scattering intensity was recorded by a two-dimensional Pilatus 300K detector, in the interval of $0.012 < q < 0.6 \text{ \AA}^{-1}$ and the wave vector was defined as:

$$q = (4\pi/\lambda) \cdot \sin(\theta/2)$$

Equation 2

where θ is the scattering angle and λ is the radiation wavelength (1.542 \AA). CPPA solutions (2mM) under study were sealed in a thin-wall quartz capillary of 1.5 mm diameter and 0.01 mm wall thickness. Measurements were performed under vacuum at ambient temperature. The scattering of the solvent was collected and subtracted from the corresponding data. Data analysis was based on fitting the scattering curve to an appropriate model by software provided by NIST (NIST SANS analysis version 6.3 on IGOR)².

S2.6 Transmission Electron Microscope (TEM) Imaging: To characterize the morphology of the CPPA assemblies, TEM imaging was performed. The TEM specimen was prepared by loading 10 μL CPPA aqueous solution with the concentration of 200 μM onto a carbon film-coated copper grid (400 mesh, Agar Scientific) and was then negatively stained for 30 s by loading 10 μL 2% (v/v) uranyl acetate solution onto the grid. The excess staining solution on the grid was removed with a piece of filter paper and the grid was then allowed to dry at room temperature for at least 3 h. Bright field TEM imaging was performed on a JEOL-1230 TEM operated at an acceleration voltage of 100 kV and the TEM images were recorded by a SIS Megaview III wide angle CCD camera.

S2.7 Zeta-potential Measurement: Zeta-potential was measured to investigate the charge of the CPPA assemblies at pH 7.4. Briefly, the CPPAs were dissolved in Milli-Q water above the CAC at 200 μM and the pH was adjusted to pH 7.4 by adding 0.1 M HCl or 0.1 M NH_4OH . The samples were measured in the Nano-ZS Zetasizer (Malvern Instruments).

S2.8 MMP-2 Cleavability Evaluation: The responsiveness of CPPAs to MMP-2 was evaluated by enzyme degradation study. Briefly, 200 μM CPPA was incubated at 37 $^\circ\text{C}$ in the presence or absence of active human MMP-2 (20 nM, reference value used to assay the MMP-2 cleavability of different peptide substrates³) in TNCB buffer (50 mM Tris-HCl, 0.15 M NaCl, 10 mM CaCl_2 , and 0.05% Brij35; pH7.4). 30 μL aliquot of the reaction mixture were sampled at time points 0 h, 0.5 h, 2 h, 6 h and 12 h, flash frozen in liquid nitrogen and stored at -20 $^\circ\text{C}$ until RP-HPLC analysis. The samples were analyzed on a Varian ProStar Model 325 HPLC system (Agilent) equipped with an analytical reverse-phase polymeric column (Varian, 100 \AA , 5 μm , 4.6 mm \times 150 mm, Agilent) using a mobile phase of $\text{H}_2\text{O}/\text{ACN}$ (0.1% TFA) under the gradient of 98% to 0% H_2O (0.1% TFA) from 0 to 18 min and detected at 220 nm. The digestion fragments were collected when significant UV signal appear and were later identified by ESI-MS. Percentage of conversion of CPPA into CPPA_{MMP} (reported as MMP-2 cleavage efficiency) was calculated by integrating the areas of corresponding peaks in the HPLC chromatograms.

S3 Supporting Figures

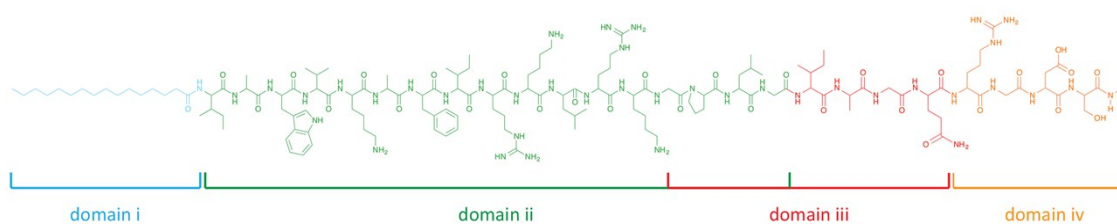


Fig. S1 Chemical structure of the rationally designed CPPA: (i) hydrophobic palmitic acid tail C16; (ii) CPP sequence; (iii) MMP-2 sensitive octapeptide linker; (iv) targeting peptide sequence.

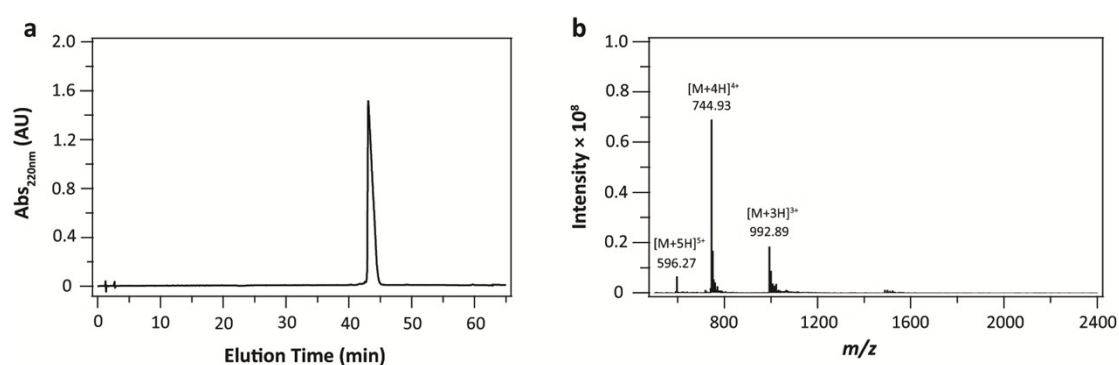


Fig. S2 Characterization of CPPA ($C_{15}H_{31}CONH-IAWVKAFIRKLRKGPLGIAGQRGDS-CONH_2$): (a) Analytical RP-HPLC chromatogram of CPPA under the gradient of 98% to 0% H_2O (0.1% TFA) from 5 to 55 min showing high purity; (b) ESI-MS spectrum of CPPA showing the expected molecular mass ($C_{141}H_{240}N_{40}O_{30}$, Mw: 2975.72 g/mol).

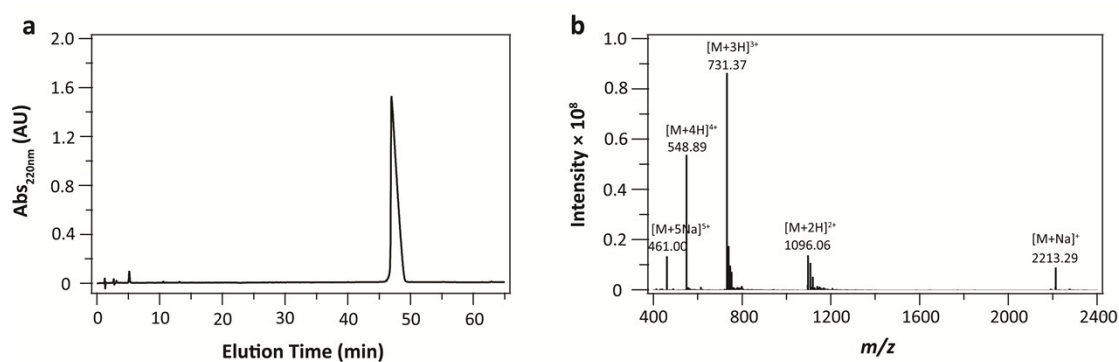


Fig. S3 Characterization of CPPA_{MMP} ($C_{15}H_{31}CONH-IAWVKAFIRKLRKGPLG-CONH_2$): (a) Analytical RP-HPLC chromatogram of CPPA_{MMP} under the gradient of 98% to 0% H_2O (0.1% TFA) from 5 to 55 min) showing high purity; (b) ESI-MS spectrum of CPPA_{MMP} showing the expected molecular mass ($C_{110}H_{188}N_{28}O_{18}$, Mw: 2190.89 g/mol).

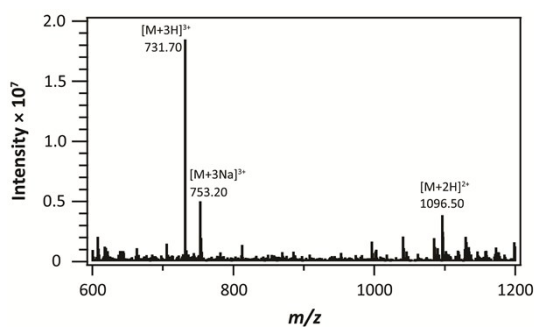


Fig. S4 Characterization of the CPPA degradation fragment: ESI-MS spectrum of the CPPA degradation fragment ($C_{15}H_{31}CONH-IAWVKAFIRKLRKGPLG-COOH$) showing the expected molecular mass ($C_{110}H_{187}N_{27}O_{19}$; Mw: 2191.88 g/mol).

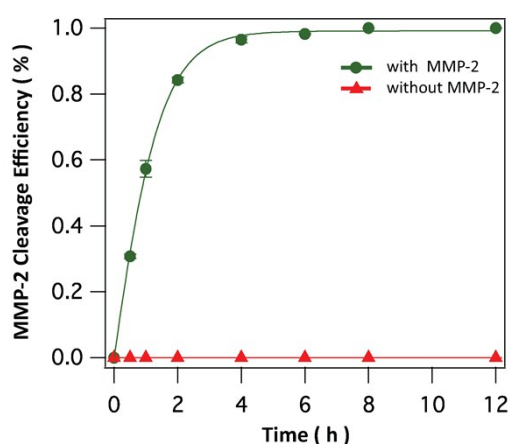


Fig. S5. MMP-2 cleavage efficiency of CPPA fibers: 200 μ M CPPA incubated with 20 nM active MMP-2 in TCNB buffer at 37 $^{\circ}$ C for different time intervals.

Table 1 Zeta-potential measurements: 200 μ M CPPA or CPPA_{MMP} in H₂O, pH 7.4

Zeta-potential (mV)	CPPA	CPPA _{MMP}
Measurement 1	63.0	83.4
Measurement 2	62.5	80.9
Measurement 3	62.9	81.2
Average	62.8 \pm 0.3	81.8 \pm 1.4

S4 References

1. M. C. A. Stuart, J. C. van de Pas and J. B. F. N. Engberts, *J Phys Org Chem*, 2005, **18**, 929-934.
2. S. R. Kline, *Journal of applied crystallography*, 2006, **39**, 895-900.
3. J. Patterson and J. A. Hubbell, *Biomaterials*, 2010, **31**, 7836-7845.